Functional Characterization of TtnD and TtnF, Unveiling New Insights into Tautomycetin Biosynthesis

Yinggang Luo,[†,||] Wenli Li,[†] Jianhua Ju,[†] Qiuping Yuan,[⊥] Noel R. Peters,[⊥] F. Michael Hoffmann,[⊥] Sheng-Xiong Huang,[†] Tim S. Bugni,[†] Scott Rajski,[†] Hiroyuki Osada,[#] and Ben Shen*,[†,§,‡]

Division of Pharmaceutical Sciences, University of Wisconsin Paul P. Carbone Comprehensive Cancer Center Small Molecule Screening Facility, University of Wisconsin National Cooperative Drug Discovery Group, and Department of Chemistry, University of Wisconsin, Madison, Wisconsin 53705-2222, Center for Natural Products Research, Chengdu Institute of Biology, Chinese Academy of Sciences, Chengdu 610041, China, and Antibiotics Laboratory, Chemical Biology Department, RIKEN Advanced Science Institute, Wako-shi, Saitama 351-0198, Japan

Received September 28, 2009; E-mail: bshen@pharmacy.wisc.edu

Abstract: The biosynthetic gene cluster for tautomycetin (TTN), a highly potent and selective protein phosphatase (PP) inhibitor isolated from *Streptomyces griseochromogenes,* has recently been cloned and sequenced. To better understand the transformations responsible for converting the post-polyketide synthase product into the exciting anticancer and immunosuppressive chemotherapeutic candidate TTN, we produced and characterized new analogues resulting from inactivation of two genes, *ttnD* and *ttnF*, in *S. griseochromogenes*. Inactivation of *ttnD* and *ttnF*, which encode for putative decarboxylase and dehydratase enzymes, respectively, afforded mutant strains SB13013 and SB13014. The ΔttnD mutant SB13013 accumulated four new TTN analogues, TTN D-1, TTN D-2, TTN D-3, and TTN D-4, whereas the ΔttnF mutant accumulated only one new TTN analogue, TTN F-1. The accumulation of these new TTN analogues defines the function of TtnD and TtnF and the timing of their chemistries in relation to installation of the C5 ketone moiety within TTN. Notably, all new analogues possess a structurally distinguishing carboxylic acid moiety, revealing that TtnD apparently cannot catalyze decarboxylation in the absence of TtnF. Additionally, cytotoxicity and PP inhibition assays reveal the importance of the functional groups installed by TtnDF and, consistent with earlier proposals, the C2″−C5 fragment of TTN to be a critical structural determinant behind the important and unique PP-1 selectivity displayed by TTN.

Introduction

Tautomycetin (TTN, **1**) and tautomycin (TTM, **2**) (Figure 1) are potent cell-permeable inhibitors of protein phosphatases (PPs) PP-1 and PP-2A and are recognized as potent inducers of apoptosis. TTN, first isolated from *Streptomyces griseochromogenes*,[1] displays nearly a 40-fold preference for PP-1 inhibition over PP-2A and is the most selective PP-1 inhibitor reported to date.[2] The PP-1 selectivity of **1** likely plays a role in the agent's extraordinary immunosuppressive activity[3] and sharply contrasts the PP-2A selective inhibition by the natural product okadaic acid, another potent phosphatase inhibitor,

making it a particularly useful tool.[4] Indeed, **1** has been instrumental in dissecting the role of PP-1 in the MEK-ERK pathway.[5] TTM, isolated from *Streptomyces spiroverticillatus*, shares significant structural features with TTN yet displays only a weak preference for PP-1 inhibition relative to PP-2A.[2]

We recently cloned and sequenced the biosynthetic gene clusters for both **1** and **2**.[6,7] In the case of the highly selective PP-1 inhibitor **1**, the *ttn* biosynthetic gene cluster from *S. griseochromogenes* was characterized and its involvement in **1** biosynthesis confirmed by gene inactivation and complementation experiments.[6] The *ttn* cluster was localized to a 79-kb DNA region, consisting of 19 open reading frames that encode two modular type I polyketide synthases (TtnAB), one type II thioesterase (TtnH), eight proteins for dialkylmaleic anhydride biosynthesis (TtnKLMNOPRS), four tailoring enzymes (Tt-

† Division of Pharmaceutical Sciences, University of Wisconsin.
‡ University of Wisconsin Paul P. Carbone Comprehensive Cancer Center Small Molecule Screening Facility.
§ University of Wisconsin National Cooperative Drug Discovery Group.
‡ Department of Chemistry, University of Wisconsin.
|| Chengdu Institute of Biology, Chinese Academy of Sciences.
RIKEN.
(1) (a) Cheng, X. C.; Kihara, T.; Ying, X.; Uramoto, M.; Osada, H.; Kusakabe, H.; Wang, B. N.; Kobayashi, Y.; Ko, K.; Yamaguchi, I.; Shen, Y. C.; Isono, K. *J. Antibiot.* **1989**, *42*, 141–144. (b) Cheng, X. C.; Kihara, T.; Kusakabe, H.; Magae, J.; Kobayashi, Y.; Fang, R. P.; Ni, Z. F.; Shen, Y. C.; Ko, K.; Yamaguchi, I.; Isono, K. *J. Antibiot.* **1987**, *40*, 907–909.
(2) Mitsuhashi, S.; Matsuura, N.; Ubukata, M.; Oikawa, H.; Shima, H.; Kikuchi, K. *Biochem. Biophys. Res. Commun.* **2001**, *287*, 328–331.

(3) Shim, J. H.; Lee, H. K.; Chang, E. J.; Chae, W. J.; Han, J. H.; Han, D. J.; Morio, T.; Yang, J. J.; Bothwell, A.; Lee, S. K. *Proc. Natl. Acad. Sci. U.S.A.* **2002**, *99*, 10617–10622.
(4) Bialojan, C.; Takai, A. *Biochem. J.* **1988**, *256*, 283–290.
(5) Lee, J. H.; Lee, J. S.; Kim, S. E.; Moon, B. S.; Kim, Y. C.; Lee, S. K.; Lee, S. K.; Choi, K. Y. *Mol. Cancer Ther.* **2006**, *5*, 3222–3231.
(6) Li, W.; Luo, Y.; Ju, J.; Rajski, S. R.; Osada, H.; Shen, B. *J. Nat. Prod.* **2009**, *72*, 450–459.
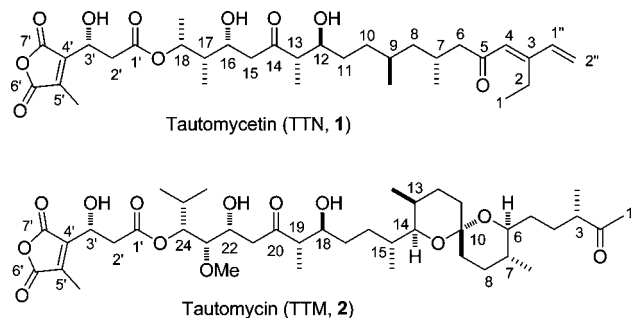(7) Li, W.; Ju, J.; Rajski, S. R.; Osada, H.; Shen, B. *J. Biol. Chem.* **2008**, *283*, 28607–28617.

Figure 1. Structures of tautomycetin (TTN, **1**) and tautomycin (TTM, **2**).

nCDFI), two regulatory proteins (TtnGQ), and one resistance protein (TtnJ). On the basis of functional assignments for each gene in the *ttn* cluster obtained from sequence analysis, we have formulated a model for biosynthesis of **1** that agrees well with previous feeding experiments, has been supported by *in vivo* gene inactivation experiments, and is supported by analogy to the recently reported *ttm* cluster. These findings set the stage to fully interrogate biosynthesis of **1**. Of particular interest is the means by which the C2″−C5 component (right hemisphere) is installed (Figure 1). This component of **1** differs significantly from the corresponding right hemisphere of **2** and has been proposed as a crucial determinant dictating the greater PP-1 selectivity of **1** relative to **2**.[8−11] This postulate has been substantiated by the recent crystal structure elucidation of PP-1 bound to **2**, although high-resolution structural information relating to PP-1 inhibition by **1** remains elusive.[12] Both **1** and

2 exist as equilibrating mixtures of anhydride and ring-opened diacids;[1b,13,14] the PP-1-to-**2** crystal structure reveals that the diacid form of **2** is the active PP-1 inhibitor and implies, by analogy, that the diacid form of anhydride **1** is the species directly responsible for PP-1 inhibition.[12]

Here, we report that inactivation of two genes, *ttnD* and *ttnF*, in *S. griseochromogenes* abolishes production of **1**, instead leading to five new analogues, TTN F-1 (**3**), TTN D-1 (**4**), TTN D-2 (**5**), TTN D-3 (**6**), and TTN D-4 (**7**), all of which lack the terminal C1″−C2″ olefin, a critical feature of the right hemisphere of **1** (Figure 2). These findings support the proposed functions of TtnF and TtnD as a dehydratase and a decarboxylase, respectively.[6] Evaluation of the cytotoxicity and PP inhibitory activities of the new analogues highlights the importance of the C2″−C5 component in providing **1** with its ability to potently inhibit PP-1 in a highly selective fashion. These data significantly improve our understanding of TTN biosynthesis and PP inhibition by TTN.

Results

Construction and Evaluation of the ΔttnD and ΔttnF Mutant Strains SB13013 and SB13014. To confirm the proposed function of TtnD and TtnF, in vivo gene inactivations were performed by using REDIRECT technology (Table S1, Supporting Information), as described previously.[6] The mutant cosmids were introduced into *S. griseochromogenes* by conjugation, and the resultant double-crossover mutants were confirmed by PCR and Southern blot analysis (Table S2, Supporting Information). Genetic complementations to the mutant strains
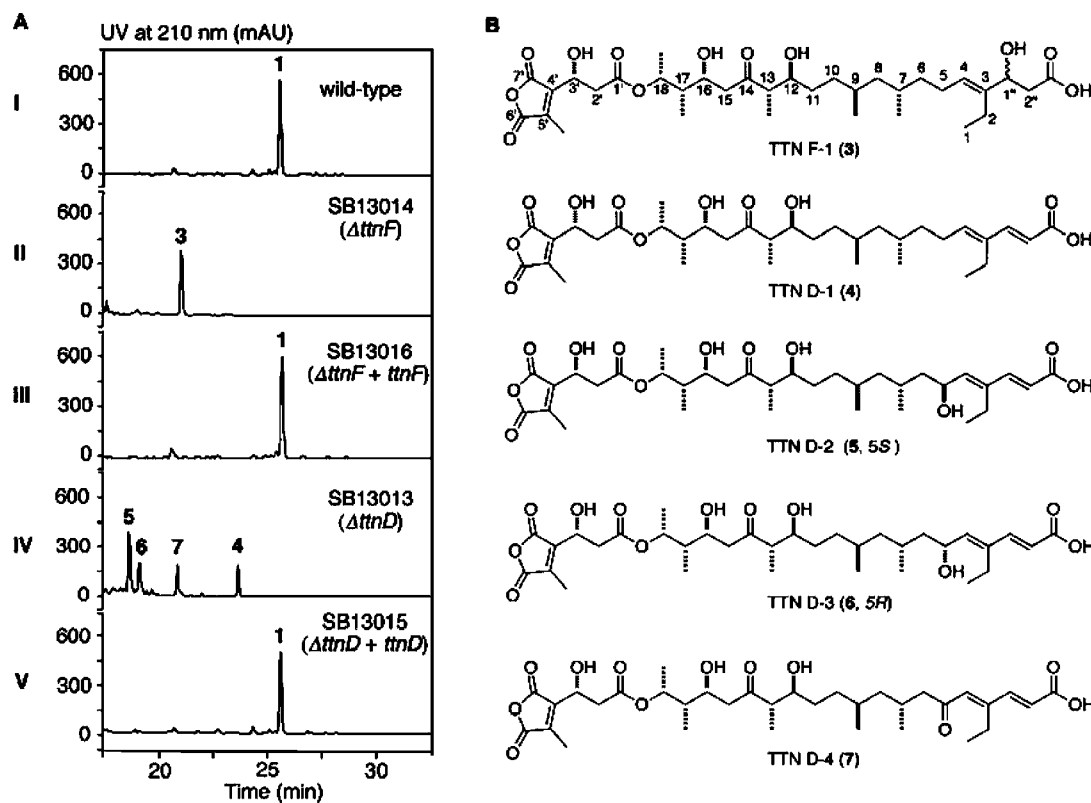

Figure 2. TTN biosynthetic intermediates and shunt metabolites accumulated in the Δ*ttnF* and Δ*ttnD* mutant strains SB13013 and SB13014. (A) HPLC traces of metabolite profiles from *S. griseochromogenes* wild-type and mutant strains: (I) *S. griseochromogenes* wild-type; (II) SB13014 (Δ*ttnF* mutant); (III) SB13016 (Δ*ttnF* complemented); (IV) SB13013 (Δ*ttnD* mutant); (V) SB13015 (Δ*ttnD* complemented). Numbers above each peak correspond to TTN (**1**), TTN F-1 (**3**), TTN D-1 (**4**), TTN D-2 (**5**), TTN D-3 (**6**), and TTN D-4 (**7**). (B) Structures of **3** from the Δ*ttnF* mutant strain SB13013 and **4**−**7** from the Δ*ttnD* mutant strain SB13014, as deduced on the basis of UV−vis, NMR, MS, and IR data.

Table 1. Summary of ^{1}H and ^{13}C NMR Data for Compounds **3**, **4**, and **7** in CDCl$_3$[a]

position	3		4		7	
	δ_H[b]	δ_C[c]	δ_H[d]	δ_C[c]	δ_H[d]	δ_C[c]
1	1.06 (3H, t, J = 7.5)	13.8	1.02 (3H, t, J = 7.6)	13.8	1.10 (3H, t, J = 7.6)	13.8
2	2.71 (2H, q, J = 7.5)	21.0	2.67 (2H, q, J = 7.2)	20.0	2.71 (2H, q, J = 7.6)	21.2
3		141.4		139.2		153.0
4	5.48 (1H, t, J = 7.0)	127.1	5.88 (1H, t, J = 7.2)	143.8	6.34 (1H, s)	132.0
5	2.10 (2H, m)	24.7	2.20 (2H, m)	26.4		201.5
6	1.19 (1H, m)	36.5	1.21 (1H, m)	37.2	2.28 (1H, dd, J = 15.6, 8.0)	53.0
	1.41 (1H, m)		1.33 (1H, m)		2.50 (1H, m)	
7	1.58 (1H, m)	28.9	1.47 (1H, m)	30.0	1.50 (1H, m)	27.4
7-CH$_3$	0.88 (3H, d, J = 6.5)	20.1	0.83 (3H, d, J = 6.4)	19.5	0.89 (3H, d, J = 6.4)	20.2
8	1.20 (2H, m)	45.3	1.09 (2H, m)	45.0	1.15 (2H, m)	45.0
9	1.54 (1H, m)	29.6	1.52 (1H, m)	30.2	1.50 (1H, m)	30.0
9-CH$_3$	0.89 (3H, d, J = 6.5)	20.3	0.86 (3H, d, J = 6.8)	19.6	0.86 (3H, d, J = 6.4)	19.5
10	1.44 (2H, m)	31.3	1.30 (2H, m)	33.1	1.30 (2H, m)	31.7
11	1.58 (2H, m)	31.2	1.52 (2H, m)	32.0	1.40 (2H, m)	32.4
12	3.82 (1H, m)	73.6	3.73 (1H, m)	74.0	3.73 (1H, m)	73.7
13	2.70 (1H, dq, J = 8.5, 7.0)	53.0	2.65 (1H, dq, J = 8.0, 7.2)	53.0	2.65 (1H, dq, J = 7.8, 7.6)	53.0
13-CH$_3$	1.12 (3H, d, J = 7.0)	14.3	1.08 (3H, d, J = 7.2)	13.6	1.08 (3H, d, J = 7.2)	13.8
14		215.9		215.9		215.9
15	2.48 (1H, dd, J = 16.5, 2.5)	46.3	2.45 (1H, dd, J = 16.8, 2.8)	46.6	2.45 (2H, m)	46.5
	2.84 (1H, dd, J = 16.5, 2.5)		2.80 (1H, dd, J = 16.8, 2.8)			
16	4.39 (1H, dt, J = 10.0, 2.5)	66.7	4.33 (1H, dt, J = 10.0, 2.0)	66.8	4.33 (1H, dt, J = 9.6, 2.4)	66.9
17	1.74 (1H, m)	43.1	1.70 (1H, m)	43.0	1.70 (1H, m)	43.0
17-CH$_3$	0.98 (3H, d, J = 6.5)	10.3	0.94 (3H, d, J = 7.2)	10.5	0.94 (3H, d, J = 7.2)	10.5
18	5.05 (1H, dq, J = 9.0, 6.5)	73.7	5.01 (1H, dq, J = 8.0, 6.4)	73.7	5.02 (1H, dq, J = 7.2, 6.4)	73.8
18-CH$_3$	1.34 (3H, d, J = 6.5)	18.6	1.29 (3H, d, J = 6.4)	18.6	1.30 (3H, d, J = 6.4)	18.6
1′		170.3		170.3		170.3
2′	2.93 (1H, dd, J = 16.0, 2.5)	40.8	2.88 (1H, dd, J = 16.0, 8.0)	40.9	2.88 (1H, dd, J = 16.0, 8.0)	40.9
	2.84 (1H, dd, J = 16.0, 4.0)		2.80 (1H, dd, J = 16.0, 4.0)		2.80 (1H, dd, J = 16.0, 4.0)	
3′	5.24 (1H, ddd, J = 9.0, 3.5, 1.0)	64.0	5.20 (1H, ddd, J = 8.0, 4.0, 1.2)	64.0	5.20 (1H, ddd, J = 8.8, 3.6, 1.2)	64.1
4′		142.4		142.4		142.3
5′		143.3		143.3		143.3
5′-CH$_3$	2.31 (3H, d, J = 1.0)	10.4	2.27 (3H, d, J = 1.2)	10.3	2.27 (3H, d, J = 1.2)	10.4
6′		165.9		165.9		165.9
7′		165.1		165.0		165.0
1″	4.49 (1H, dd, J = 7.5, 4.5)	71.8	7.28 (1H, d, J = 15.2)	151.0	7.23 (1H, d, J = 16.0)	148.8
2″	2.60 (2H, m)	40.5	5.78 (1H, d, J = 15.2)	114.3	6.26 (1H, d, J = 16.0)	122.8
3″		175.4		172.3		170.4

[a] Chemical shifts are reported in ppm, coupling constants (J) in hertz. All signals are determined by ^{1}H–^{1}H COSY, HSQC, and HMBC correlations. [b] ^{1}H NMR, 500 MHz. [c] ^{13}C NMR, 100 MHz. [d] ^{1}H NMR, 400 MHz.

were subsequently carried out to eliminate the possibility of polar effects (Table S3, Supporting Information).

Isolation and Characterization of TTN Analogue 3 from SB13014 and TTN Analogues 4−7 from SB13013. Mutant strains SB13013 (ΔttnD) and SB13014 (ΔttnF) were fermented according to TTN production methods previously reported for the *S. griseochromogenes* wild-type strain, and corresponding metabolites were analyzed by HPLC with authentic TTN as a control.[6] Only one TTN analogue **3** was accumulated and isolated from the ΔttnF mutant strain SB13014 (Figure 2). Its molecular formula, $C_{34}H_{54}O_{12}$, was established from the quasi-molecular ion at m/z 653.3532 ([M − H]$^-$), requiring an additional CH_4O_2 moiety relative to **1**. Instead of the C2″−C5 moiety present in the right fragment of **1**, only one trisubstituted olefin was deduced in **3** on the basis of characteristic NMR signals at δ_H 5.48 (1H, t, J = 7.0 Hz), δ_C 127.1 (d), and δ_C

141.4 (s) (Table 1). Two substituted groups, one β-hydroxypropanoic acid moiety (C1″−C3″) and one ethyl moiety (C1−C2), were observed in the 1-D and 2-D NMR data with connectivity to the carbon observed at 141.4 ppm (s, C-3) of the only double bond (Table 1). The third substituent of this double bond was assigned as a methylene group in view of the characteristic ^{1}H NMR triplet signal observed at δ_H 5.48 (1H, t, J = 7.0 Hz). This assignment was confirmed by HMQC and HMBC signals (Figure 3A). Thus, the C5 of **3** was assigned as a methylene group and not a ketone. The upfield NMR signals were consistent with those previously observed for **1** and were assigned on the basis of 2-D NMR cross signals (Table 1 and Figure 3A). The stereochemical configurations at C7, C9, C12, C13, C16, C17, C18, and C3′ are suggested to be identical to those of **1** on the basis of their shared biosynthetic origin and the very similar optical rotations observed for **1** and **3**. Although we could predict an *R*-configuration for C1″ of **3** on the basis of bioinformatics comparisons of conserved amino acid residues of the TTN polyketide synthase KR domain and those of KR domains associated with stereochemically defined natural products,[15] the absolute stereochemistry was not established experimentally. Attempts to make the Mosher ester of **3** were

(8) Oikawa, H. *Curr. Med. Chem.* **2002**, *9*, 2033–2054.
(9) Nishiyama, U.; Ubukata, M.; Magae, J.; Kataoka, T.; Erdoedi, F.; Hartshorne, D. J.; Isono, K.; Nagai, K.; Osada, H. *Biosci. Biotechnol. Biochem.* **1996**, *60*, 103–107.
(10) Sheppeck, J. E., II; Liu, W.; Chamberlin, A. R. *J. Org. Chem.* **1997**, *62*, 387–398.
(11) Takai, A.; Tsuboi, K.; Koyasu, M.; Isobe, M. *Biochem. J.* **2000**, *350*, 81–88.
(12) Kelker, M. S.; Page, R.; Peti, W. *J. Mol. Biol.* **2009**, *385*, 11–21.
(13) Cheng, X. C.; Ubukata, M.; Isono, K. *J. Antibiot.* **1990**, *43*, 890–896.
(14) Cheng, X. C.; Ubukata, M.; Isono, K. *J. Antibiot.* **1990**, *43*, 809–819.
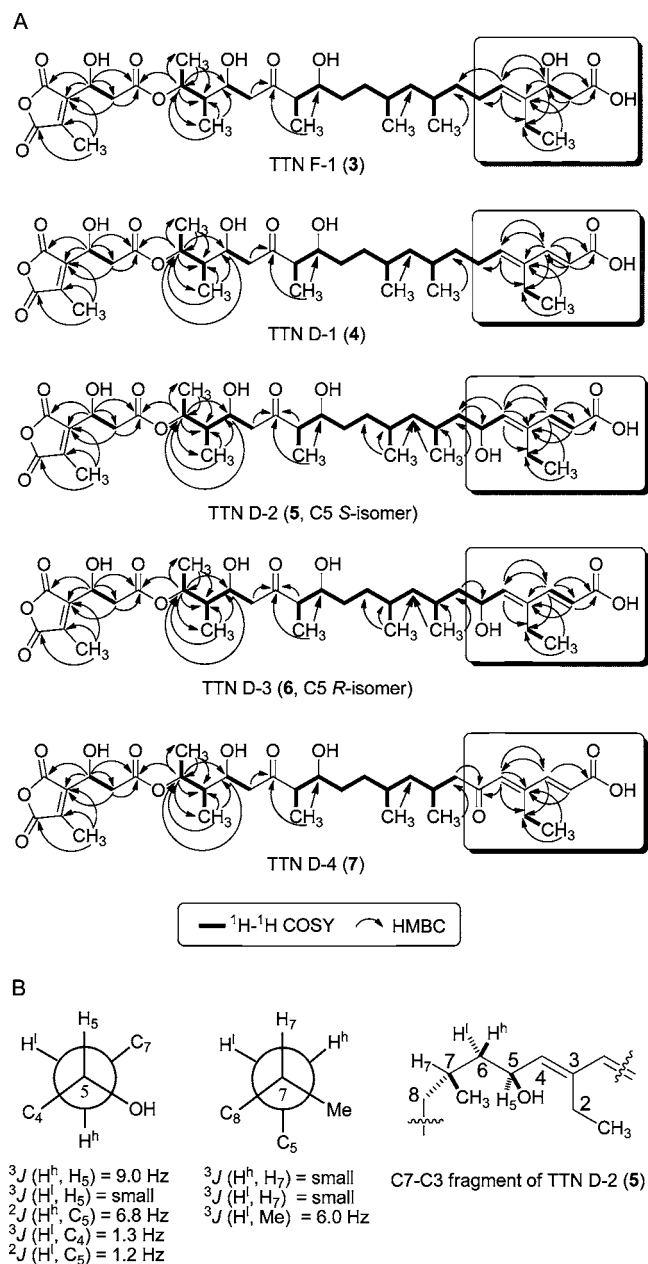
(15) Keatinge-Clay, A. T. *Chem. Biol.* **2007**, *14*, 898–908.

A

TTN F-1 (**3**)

TTN D-1 (**4**)

TTN D-2 (**5**, C5 *S*-isomer)

TTN D-3 (**6**, C5 *R*-isomer)

TTN D-4 (**7**)

— ¹H-¹H COSY   ⌢ HMBC

B

³*J* (H^l, H₅) = 9.0 Hz
³*J* (H^l, H₅) = small
²*J* (H^h, C₅) = 6.8 Hz
³*J* (H^l, C₄) = 1.3 Hz
²*J* (H^l, C₅) = 1.2 Hz

³*J* (H^h, H₇) = small
³*J* (H^l, H₇) = small
³*J* (H^l, Me) = 6.0 Hz

C7-C3 fragment of TTN D-2 (**5**)

Figure 3. (A) Key ¹H–¹H COSY and HMBC correlations observed and applied to structure determination for TTN analogues **3**–**7**. (B) Determination of the *S*-configuration at C5 of **5** on the basis of HETLOC, gHSQMBC, and gDQCOSY analyses.

unsuccessful, with **3** undergoing rapid dehydration to **4** under all conditions examined.[16]

Four TTN analogues, **4**–**7**, were accumulated and isolated from the Δ*ttnD* mutant strain SB13013 (Figure 2). Their structures were elucidated on the basis of 1-D and 2-D NMR (including ¹H and ¹³C NMR, ¹H–¹H COSY, HMQC, and HMBC data), UV, IR, and HRMS data. The molecular formula of **4**, $C_{34}H_{52}O_{11}$, was established from the quasi-molecular ion at *m/z* 659.3412 ([M + Na]⁺), requiring one H₂O less than **3**. The only difference between **4** and **3** was that **4** is not a β-hydroxypropanoic acid moiety but rather an acrylic acid moiety attached to C3, as deduced from its 1-D and 2-D NMR

data (Table 1). The characteristic coupling constant 15.2 Hz between the two protons at δ_H 7.28 and 5.78 (each 1H, d, *J* = 15.2) suggests a *trans*-double bond within the acrylic acid moiety (Table 1). The upfield NMR signals were consistent with those of **3** and were assigned by 2-D NMR cross signals (Table 1 and Figure 3A). Stereochemical configurations at C7, C9, C12, C13, C16, C17, C18, and C3′ are predicted to be identical to those of **1** on the basis of the shared biosynthetic origin of **1** and **4**.

The molecular formula of **5**, $C_{34}H_{52}O_{12}$, was established from the quasi-molecular ion at *m/z* 651.3400 ([M − H]⁻), requiring one more oxygen atom than **4**. The only difference between **5** and **4** was that the characteristic ¹H NMR signal of the proton of C4 is a doublet at δ_H 5.77 (1H, d, *J* = 8.8 Hz), instead of the triplet signal observed in **3** and **4**. Thus, C5 was assigned as a methine group instead of a methylene moiety, which is the case for **3** and **4**. In view of the NMR signals at δ_H 4.58 (1H, m) and δ_C 66.6 (d), the oxygenation at C5 was deduced. C5 oxygenation was confirmed by ¹H–¹H COSY, HMQC, and HMBC cross signals (Table 2 and Figure 3A). The upfield NMR signals were consistent with those of **4** and were assigned by 2-D NMR cross signals (Table 2 and Figure 3A). Stereochemical configurations spanning C3′ to C7 (with the exception of C5) were assigned in a fashion analogous to that used for compounds **3** and **4**.

The molecular formula of **6**, $C_{34}H_{52}O_{12}$, deduced on the basis of the quasi-molecular ion at *m/z* 651.3399 ([M − H]⁻), is identical to that of **5**. The NMR spectra of **5** and **6** were almost superimposable (Table 2 and Figure 3A). The only discernible difference between the two compounds was their ¹H and ¹³C NMR signals around C5, suggestive of a diastereomeric relationship between **5** and **6**, the result of opposite configurations at C5. The exact configuration at C5 for **5** was subsequently assigned on the basis of extensive HETLOC, gHSQM-BC, and gDQCOSY experiments.[17,18] Thus, the anti orientation of H^h-6/H-5 was suggested by the observed large ³*J* value (9.0 Hz), while the gauche orientations of H^l-6/H-5, H^l-6/H-7, and H^h-6/H-7 were supported by the small ³*J* values. The anti orientations of H^l-6/OH and H^l-6/7-Me were shown by the small ²*J* value for H^l-6/C5 and the large ³*J* value (6.0 Hz) for H^l-6/7-Me, respectively. The gauche orientation of H^h-6/5-OH was suggested by the large ²*J* value (6.8 Hz) (Figure 3B). Taken together, an *S*-configuration was assigned to C5 of **5**, and thereby an *R*-configuration at C5 for **6** on the basis of their diastereomeric relationship (Table 2 and Figure 2B).

For **7**, a molecular formula of $C_{34}H_{50}O_{12}$ was established from the quasi-molecular ion at *m/z* 649.3219 ([M − H]⁻), requiring two protons less than **5**. The only difference between **7** and **5** was that the characteristic ¹H resonance for the C4 proton in **7** was a singlet at δ_H 6.34 (1H, s), instead of a triplet as observed for **3** and **4**, or a doublet as observed for **5** and **6**. The suggestion, on the basis of these data, that C5 of **7** was a carbonyl carbon was prompted by the observed ¹³C NMR signal at δ_C 201.5 (s), indicative of a quaternary carbon. The identity of C5 in **7** as a ketone carbon was confirmed by HMBC cross signals (Table 1 and Figure 3A) and is the only significant structural difference between **7** and its putative methylene precursor compound **4** (Figure 2B). The upfield NMR signals for **7** were consistent with those of **1** and its analogues and were assigned by 2-D

(16) (a) Dale, J. A. H.; Mosher, S. *J. Am. Chem. Soc.* **1973**, *95*, 512–519. (b) Ohtani, I.; Kusumi, T.; Kashman, Y.; Kakisawa, H. *J. Am. Chem. Soc.* **1991**, *113*, 4092–4096.

(17) Uhrín, D.; Batta, G.; Hruby, V. J.; Barlow, P. N.; Kövér, K. E. *J. Magn. Reson.* **1998**, *130*, 155.
(18) Williamson, R. T.; Márquez, B. L.; Gerwick, W. H.; Kövér, K. E. *Magn. Reson. Chem.* **2000**, *38*, 265.

Table 2. Summary of ¹H and ¹³C NMR Data for Compounds **5** and **6** in CDCl₃[a]

position	**5** δ$_H$[b]	δ$_C$[c]	**6** δ$_H$[b]	δ$_C$[c]
1	1.07 (3H, t, *J* = 7.2)	13.8	1.05 (3H, t, *J* = 7.6)	13.8
2	2.32 (2H, q, *J* = 7.2)	20.4	2.30 (2H, q, *J* = 7.6)	20.4
3		140.2		140.2
4	5.77 (1H, d, *J* = 8.8)	143.3	5.82 (1H, d, *J* = 8.8)	143.6
5	4.58 (1H, m)	66.6	4.56 (1H, m)	66.5
6	1.18, 1.47 (each 1H, m)	45.0	1.10, 1.67 (each 1H, m)	45.6
7	1.57 (1H, m)	26.7	1.75 (1H, m)	26.5
7-CH₃	0.89 (3H, d, *J* = 6.4)	21.0	0.93 (3H, d, *J* = 6.4)	20.3
8	1.08, 1.17 (each 1H, m)	45.3	1.05, 1.16 (each 1H, m)	44.6
9	1.40 (1H, m)	32.1	1.55 (1H, m)	31.4
9-CH₃	0.84 (3H, d, *J* = 6.4)	19.7	0.84 (3H, d, *J* = 6.4)	20.1
10	1.28 (2H, m)	29.8	1.28 (2H, m)	29.2
11	1.38 (2H, m)	31.7	1.38 (2H, m)	31.5
12	3.75 (1H, m)	73.6	3.78 (1H, dt, *J* = 8.8, 2.4)	73.2
13	2.64 (1H, dq, *J* = 7.6, 7.2)	53.1	2.65 (1H, dq, *J* = 7.6, 7.2)	52.9
13-CH₃	1.08 (3H, d, *J* = 7.2)	14.2	1.07 (3H, d, *J* = 7.2)	14.0
14		215.8		215.8
15	2.79 (1H, dd, *J* = 16.4, 6.0)	46.4	2.79 (1H, dd, *J* = 16.8, 6.0)	46.7
	2.44 (1H, dd, *J* = 16.4, 2.4)		2.46 (1H, dd, *J* = 16.8, 2.4)	
16	4.35 (1H, dt, *J* = 9.6, 2.4)	66.7	4.35 (1H, dt, *J* = 10.0, 2.4)	66.7
17	1.70 (1H, m)	43.1	1.70 (1H, m)	43.1
17-CH₃	0.94 (3H, d, *J* = 6.8)	10.4	0.93 (3H, d, *J* = 6.8)	10.4
18	4.99 (1H, dq, *J* = 7.2, 6.0)	73.7	4.98 (1H, dq, *J* = 7.2, 6.0)	73.7
18-CH₃	1.29 (3H, d, *J* = 6.4)	18.6	1.28 (3H, d, *J* = 6.4)	18.6
1′		170.3		170.2
2′	2.88 (1H, dd, *J* = 16.4, 4.4)	40.9	2.88 (1H, dd, *J* = 16.0, 4.0)	40.9
	2.80 (1H, dd, *J* = 16.4, 9.2)		2.80 (1H, dd, *J* = 16.0, 8.8)	
3′	5.19 (1H, ddd, *J* = 7.6, 4.0, 1.2)	63.9	5.19 (1H, ddd, *J* = 7.2, 4.0, 1.2)	63.9
4′		142.4		142.4
5′		143.1		143.2
5′-CH₃	2.26 (3H, d, *J* = 0.8)	10.3	2.26 (3H, d, *J* = 1.2)	10.3
6′		166.0		166.0
7′		165.1		165.1
1″	7.25 (1H, d, *J* = 16.0)	149.8	7.24 (1H, d, *J* = 16.0)	149.8
2″	5.90 (1H, d, *J* = 16.0)	117.0	5.89 (1H, d, *J* = 16.0)	116.9
3″		170.9		171.2

[a] Chemical shifts are reported in ppm, coupling constants (*J*) in hertz. All signals are determined by ¹H–¹H COSY, HSQC, and HMBC correlations. [b] ¹H NMR, 400 MHz. [c] ¹³C NMR, 100 MHz.

Table 3. Summary of in Vitro Inhibition Data (IC₅₀ in μM) for TTN and Analogues against PP-1 and PP-2

compound	PP-1	PP-2A	PP-1/PP-2A
TTN (**1**)	15 ± 0.8 × 10⁻³	0.40 ± 0.04	1:27
TTN F-1 (**3**)	0.17 ± 0.01	0.64 ± 0.08	1:3.8
TTN D-1 (**4**)	0.13 ± 0.02	0.52 ± 0.05	1:4
TTN D-2 (**5**)	9.8 ± 0.1	44 ± 0.1	1:4.5
TTN D-3 (**6**)	0.21 ± 0.03	0.80 ± 0.06	1:3.8
TTN D-4 (**7**)	0.28 ± 0.02	0.92 ± 0.04	1:3.3

Table 4. Summary of in Vitro Cytotoxicity Data (IC₅₀ in μM) for TTN and Analogues against Selected Human Cancer Cell Lines

compound	Du145	MCF7	HCT-115
TTN (**1**)	5.2 ± 0.4	8.9 ± 0.9	6.8 ± 0.6
TTN F-1 (**3**)	nd[a]	nd	nd
TTN D-1 (**4**)	nd	nd	nd
TTN D-2 (**5**)	nd	nd	nd
TTN D-3 (**6**)	14 ± 3	11 ± 3	16 ± 3
TTN D-4 (**7**)	13 ± 4	17 ± 3	18 ± 3

[a] nd, no significant activity detected.

NMR cross signals (Table 1 and Figure 3A). Stereochemical configurations at C7, C9, C12, C13, C16, C17, C18, and C3′ in **7** are likely identical to those observed in **1** on the basis of the compounds' shared biosynthetic origin.

Evaluation of PP Inhibitory Activity and Cytotoxicity of 3–7 in Comparison with 1. Compounds **3–7** were subjected to PP inhibition and cytotoxicity assays with **1** as a control.[19] Assays focused specifically on the inhibition of PP-1 and PP-2A (Table 3), while cytotoxicity assays exploited the use of selected human cancer cell lines Du145, MCF7, and HCT-115 (Table 4).

Discussion

The C2″–C5 fragment of **1** is not consistent with structural expectations for the nascent polyketide resulting from the TtnAB polyketide synthase as predicted previously.[6] The involvement

of post-polyketide synthase steps en route to **1** was supported by the presence of four genes associated with putative tailoring enzymes: TtnC, a flavoprotein decarboxylase homologue; TtnD, a UbiD family decarboxylase homologue; TtnF, an L-carnitine dehydratase homologue; and TtnI, a putative cytochrome P450.[6] On the basis of these functional assignments and the predicted synthetic capabilities of the TtnAB polyketide synthases, we have previously proposed **1** to arise through the intermediacy of a β-hydroxy acid intermediate (Figure 4).[6] Concomitant decarboxylation and dehydration to form the terminal olefin has been previously suggested,[17,18] and olefin installation in this manner was postulated to benefit substantially from the presence of the C5 ketone and its conjugation with the C3–C4 olefin.

(19) Ju, J.; Li, W.; Yuan, Q.; Peters, N. R.; Hoffmann, F. M.; Rajski, S. R.; Osada, H.; Shen, B. *Org. Lett.* **2009**, *11*, 1639–1642.
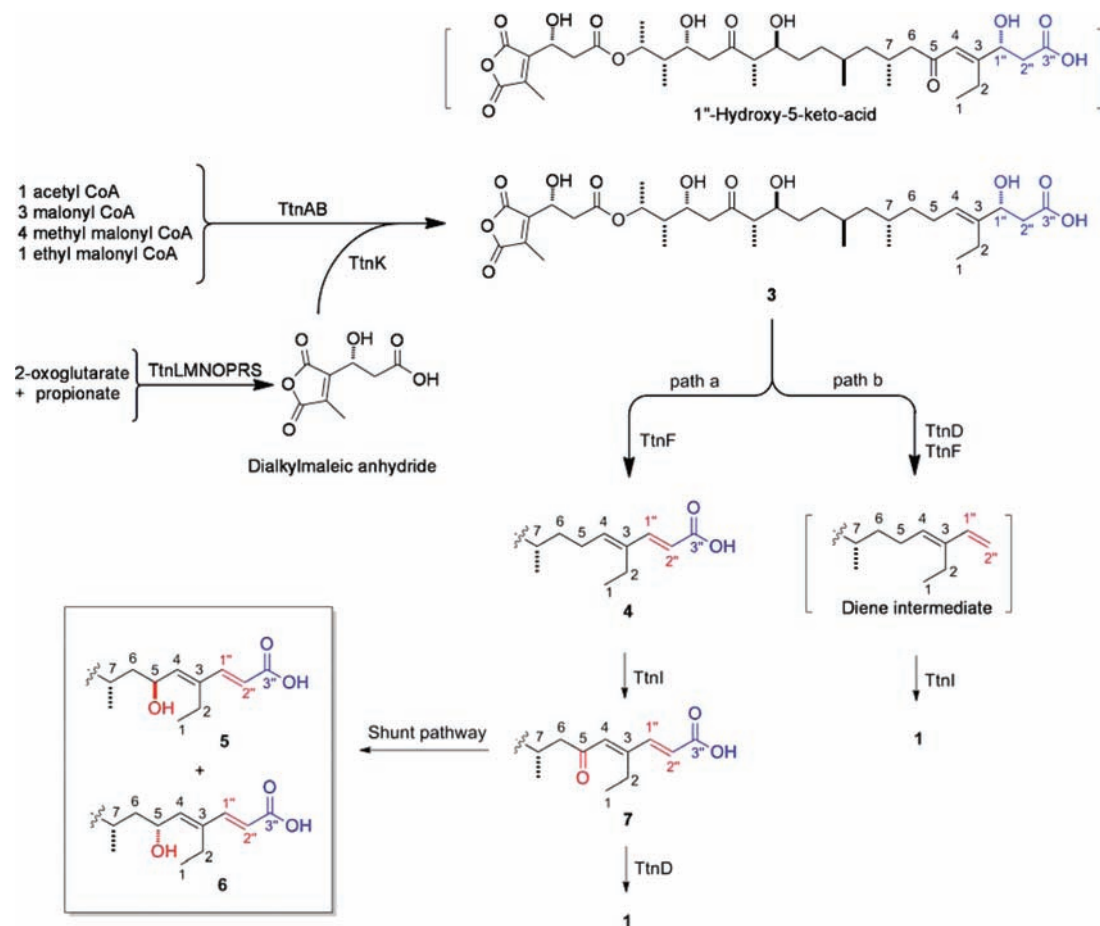
Figure 4. Proposed biosynthesis of **1** predicated on a linear biosynthetic logic leading to intermediate **3** and subsequent processing by tailoring enzymes TtnD and TtnF. Tailoring steps involving TtnF, TtnI, and TtnD and their ordering are assigned on the basis of metabolites **3–7** accumulated by ΔttnD and ΔttnF mutant strain SB13013 and SB13014s. We envision TtnI as a C5 oxidase on the basis of its similarity to cytochrome P450 hydroxylases. In proceeding from **3**, path a invokes the sequential actions of TtnF, TtnI, and TtnD with **5** and **6** most likely derived by adventitious reduction of **7**. Path b invokes coordinated activity by both TtnD and TtnF to produce a diene intermediate, which is subsequent oxidized at C5 by TtnI to afford **1**. Molecular fragments not shown are identical to those of their putative precursor **3**. The current studies disprove the intermediacy of 1″-hydroxy-5-keto acid in **1** biosynthesis proposed previously.[6]

The true functions of putative dehydratase TtnF and decarboxylase TtnD were evaluated using gene inactivation strategies followed by examining metabolite profiles of the resultant mutant strains. It is significant to note that under no circumstances was the previously postulated β-hydroxy acid intermediate observed, and this finding is consistent with the alternative idea that C5 oxidation proceeds after the chemistries of TtnD and TtnF (Figure 4). The ΔttnF mutant SB13014 accumulated **3**, whereas the ΔttnD mutant SB13013 accumulated compounds **4–7**. The accumulation of **3** in the ΔttnF mutant reveals three important details about the biosynthesis of **1** (Figure 2). First, it confirms the functional assignment of TtnF as a dehydratase. Second, and perhaps more surprising, is that retention of the terminal acid in **3** suggests that the decarboxylase activity of TtnD requires the presence of TtnF; TtnD alone is not sufficient to effect decarboxylation. Conventional reactivity considerations

dictate that dehydration of the allylic C1″ in **3** or related compounds might occur upon TtnD-catalyzed decarboxylation. However, the accumulation of **3** in the presence of TtnD but the absence of TtnF reveals the flaw in this thinking, as does the fact that no trace of **1**, **4**, **5**, **6**, or **7** could be found in fermentations of the ΔttnF mutant SB13014. The biosynthetic transformations catalyzed by TtnD and TtnF appear to occur in concert. Conversely, TtnF-catalyzed dehydration of C1″ is in no way dependent upon the decarboxylase activity of TtnD, as reflected by the absence of the C1″ OH moiety in all compounds accumulated by the ΔttnD mutant SB13013. Third, the accumulation of **3** by ΔttnF mutant SB13014 reveals that dehydration chemistry precedes polyketide C-5 oxidation needed for ketone installation. This is not the case for the ΔttnD mutant SB13013, which accumulated the C5 ketone **7** in addition to compounds **4–6**. TtnI, a cytochrome P450 homologue, the only oxygenase within the *ttn* cluster and a putative C5 oxidase, is likely responsible for conversion of **4** into **7**. That **4–6**, and not just **7**, accumulate in SB13013 suggests that the ΔttnD mutant accumulates impaired TtnI substrates. It is clear that the activities of TtnD, TtnF, and TtnI are, to varying extents, impacted by the chemistries catalyzed by each other.

The accumulation of **3** by the ΔttnF mutant SB13014 and of **4–7** by the ΔttnD mutant SB13013 allows us to more accurately

(20) Chang, Z. X.; Sitachitta, N.; Rossi, J. V.; Roberts, M. A.; Flatt, P. M.; Jia, J. Y.; Sherman, D. H.; Gerwick, W. H. *J. Nat. Prod.* **2004**, *67*, 1356–1367.

(21) Gu, L.; Wang, B.; Kulkarni, A.; Gehret, J. J.; Lloyd, K. R.; Gerwick, L.; Gerwick, W. H.; Wipf, P.; Hakansson, K.; Smith, J. L.; Sherman, D. H. *J. Am. Chem. Soc.* **2009**, *131*, 16033–16035.

(22) Zhang, J.; Van Lanen, S. G.; Ju, J.; Liu, W.; Dorrestein, P. C.; Li, W.; Kelleher, N. L.; Shen, B. *Proc. Natl. Acad. Sci. U.S.A.* **2008**, *105*, 1460–1465.

predict the biosynthesis of **1** (Figure 4). Previous inactivation experiments indicate that TTN biosynthesis proceeds by a linear pathway.[6] The dialkylmaleic anhydride unit is coupled to the growing TTN polyketide intermediate prior to its release from the polyketide synthase, with the dialkylmaleic anhydride being constructed via an independent pathway that relies on TtnLM-NOPRS.[6] Hence, we envision a biosynthetic pathway in which acetyl CoA, malonyl CoA, methylmalonyl CoA, and ethylmalonyl CoA are used by the two polyketide synthases TtnAB to produce, after TtnK-mediated dialkylmaleic anhydride coupling, **3** (Figure 4). The absence of any C5 oxygenated analogues of **3** accumulated by the Δ*ttnF* mutant SB13014 suggests that TtnF-catalyzed chemistry precedes that of TtnI, an observation leading us now to postulate that, once formed, **3** is dehydrated by TtnF to provide diene **4**.[6] The findings would also be consistent with an alternative scenario wherein TtnF and TtnD act in concert to produce a diene intermediate, a substrate then for C5 oxidation by TtnI (Figure 4). Both biosynthetic hypotheses for ultimate conversion of **3** to **1** relegate C5 oxidation to a late-stage transformation, although further inactivation efforts are warranted to determine the precise timing and coordination of the steps catalyzed by TtnF, TtnI, and TtnD. Finally, the accumulation of C5 alcohols **5** and **6** in the Δ*ttnD* mutant SB13013 could have resulted from C5 oxidation of compound **4** or C5 reduction of compound **7** by adventitious enzymes. However, regardless of the precise means by which **5** and **6** are produced, that both stereoisomers at C5 are observed correlates well with the production of **5** and **6** as shunt metabolites rather than intermediates formed by the stereospecific biosynthetic machinery driving production of **1**.

A critical distinction between **1** and **2** is the significantly greater selectivity of **1** for inhibition of PP-1 over PP-2A relative to **2**.[8-11] Yet surprisingly, little attention has been directed to the generation of TTN analogues able to give insight into the structural basis for this selectivity; **3**–**7** are among the first TTN analogues reported. In light of extensive efforts to produce analogues of **2** as possible drug candidates, the lack of interest in analogue generation with **1** is truly remarkable.[8-11,23-26] To investigate the impact of right hemisphere modification upon TTN bioactivity, **1** and **3**–**7** were subjected to PP inhibition and cytotoxicity assays as previously described.[6] Assays focused specifically on the inhibition of PP-1 and PP-2A, while cytotoxicity assays exploited the use of selected human cancer cell lines Du145, MCF7, and HCT-115.[19] Thus, as summarized in Table 4, the impact of right hemisphere modifications on cytotoxicity appeared mixed. While the new analogues **3**, **4**, and **5** were inactive, **6** and **7** retained significant, albeit reduced, cytoxicity (within 3-fold of reduction relative to **1**). In contrast, modifications of the right hemisphere of **1** clearly had a profound, uniform impact on its PP-1 selectivity. As shown in Table 3, **1** potently inhibited both PP-1 and PP-2 and did so with a PP-1 selectivity of about 27-fold. Analogues **3**, **4**, **6**, and **7** inhibited PP-1 less efficiently than **1** by approximately 1 order of magnitude yet inhibited PP-2A with about the same potency as **1**. In effect, any change to the C2″−C5 portion of **1** led to a significant decrease in PP-1-selective inhibition, a key

trademark of **1**. Not only was this the case for **3**, **4**, **6**, and **7**, but this was observed also for **5**, which was a significantly poorer PP inhibitor than any other right hemisphere congener tested. PP-1 inhibition by **5** was approximately 3 orders of magnitude worse than that by **1**, and PP-2A inhibition by **5** was about 2 orders of magnitude worse than that by **1**. Hence, although the PP-1 selectivity of **5** is on par with that of all other analogues tested, the absolute inhibitory activity of **5** was markedly less than those of all the other analogues, even its diastereomer **6**. The precise molecular origins of the more dramatically altered activity of **5** relative to other TTN analogues are uncertain. However, the results of these studies support proposals implicating the right hemisphere of **1** as providing much of the compound's PP-1 selectivity relative to PP-2A.[8-11]

Taken together, our ability to correlate inactivation of the *ttnD* and *ttnF* genes with specific structural modifications to **1** supports the significance of the genetic system developed for the TTN producer *S. griseochromogenes* during sequencing of the *ttn* biosynthetic gene cluster and reinforces current functional assignments for all genes in the *ttn* cluster. The accumulation of compounds **3**–**7** in Δ*ttnD* and Δ*ttnF* mutant strains SB13013 and SB13014 gives significant new insight into how the C2″−C5 fragment of **1** is produced and how these chemistries might be applied in a combinatorial biosynthetic fashion to produce new analogues of **1**. Production of **3**–**7** has also allowed us to critically evaluate some of the structural determinants responsible for the PP-1 selectivity of **1** relative to other PP inhibitors and general cytotoxicites against selected human cancer cells. These data establish an excellent stage for future investigations of TTN biosynthesis and the future generation of TTN analogues by manipulating the **1** biosynthetic machinery.

Experimental Procedures

General. IR spectra were measured on a Bruker EQUINOX 55/S FT-IR/NIR spectrophotometer (Ettlingen, DE). Optical rotations were determined on a Perkin-Elmer 241 instrument at the sodium D line (589 nm). High-resolution mass spectrometry (HRMS) analyses were acquired on an IonSpec HiRes MALDI FT mass spectrometer (Lake Forest, CA) for HRMALDIMS or on an Agilent 1100 series LC/MSD Trap SL for HRESIMS (Santa Clara, CA). NMR data were recorded on a Varian Unity Inova 400 or 500 MHz NMR spectrometer (Varian, Inc., Palo Alto, CA). ^{1}H and ^{13}C NMR chemical shifts were referenced to residual solvent signals: δ_H 7.26 ppm and δ_C 77.7 ppm for CDCl$_3$. [1]H−^{1}H COSY, HMQC, HMBC, HETLOC, gHSQMBC, and gDQCOSY were performed using either standard Varian pulse sequences or literature pulse sequences.[17,18] High-performance liquid chromatography (HPLC) analysis was carried out on a Varian HPLC system equipped with ProStar 210 pumps and a photodiode detector. Mobile phases used were buffer A (H$_2$O) and buffer B (CH$_3$CN). Analytical and semi-preparative HPLC columns used were Alltech Alltima C18 columns, 250 × 4.6 mm, 5 μm and 250 × 10 mm, 5 μm, respectively. Cytotoxity assays and PP inhibition assays for TTN and related analogues were performed as previously described for compound **2** and related congeners.[19] Medium components and all other chemical solvents and reagents were purchased from Fisher Scientific (Fairlawn, NJ). Silica gel 60 RP-18 (230−400 mesh, EMD Chemical Inc., Gibbstown, NJ) was used for standard benchtop column chromatography. Amberlite XAD-16 resin was purchased from Sigma.

Bacterial Strains and Plasmids. *Escherichia coli* DH5α was used as the host for general subcloning.[27] *E. coli* ET12567/

(23) Liu, W.; Sheppeck, J. E., II; Colby, D. A.; Huang, H.-B.; Nairin, A. C.; Chamberlin, A. R. *Bioorg. Med. Chem. Lett.* **2003**, *13*, 1597–1600.
(24) Oikawa, H.; Yoneta, Y.; Ueno, T.; Oikawa, M.; Wakayama, T.; Ichihara, A.; Kawamura, T.; Matsuzawa, S.-I.; Kikuchi, K. *Tennen Yuki Kagobutsu Toronkai Koen Yoshishu* **1997**, *39*, 433–438.
(25) Isobe, M. *Yuki, Gosei Kagaku Kyokaishi* **1997**, *55*, 60–71.
(26) Oikawa, H.; Oikawa, M.; Ichihara, A.; Ubukata, M.; Isono, K. *Biosci. Biotechnol. Biochem.* **1994**, *58*, 1933–1935.

(27) Sambrook, J. E.; Fritsch, E. F.; Maniatis, T. *Molecular cloning: a Laboratory Manual*, 3rd Ed.; Cold Spring Harbor Laboratory Press: Cold Spring Harbor, NY, 2000.

pUZ8002[28] was used as the cosmid donor host for *E. coli*−*Streptomyces* conjugation. *E. coli* BW25113/pIJ790 and *E. coli* DH5α/pIJ773 were provided by John Innes Center (Norwich, UK) as a part of the REDIRECT Technology kit.[29] The *S. griseochromogenes* wild-type strain has been described previously.[1b,14]

Biochemicals, Chemicals, and Media. Common biochemicals and chemicals were from standard commercial sources. *E. coli* strains carrying plasmids were grown in Luria−Bertani (LB) medium with appropriate antibiotics selection.[27] All media for *Streptomyces* growth were prepared according to standard protocols.[30] ISP-4 and tryptic soy broth (TSB) were from Difco Laboratories (Detroit, MI), and modified ISP-4 is ISP-4 supplemented with 0.05% yeast extract and 0.1% tryptone.[31] ISP-4 medium and MS medium were used for *S. griseochromogenes* sporulation at 30 °C for 5−7 days.

S. griseochromogenes Strain Sporulation and Growth Conditions. The *S. griseochromogenes* wild-type and Δ*ttnD* and Δ*ttnF* mutant strains SB13013 and SB13014 were grown on MS medium (consisting of autoclaved 2% mannitol, 3% soybean flour, and 1.8% agar in tap water) at 30 °C until they were well sporulated (7 days). Spores were then harvested and stored in 20% glycerol at −80 °C using previously reported standard procedures.

Plasmids and DNA Manipulation. Plasmid extraction and DNA purification were carried out using commercial kits (Qiagen, Santa Clarita, CA) and genomic DNAs isolated according to literature protocol.[30] The digoxigenin-11-dUTP labeling and detection kit (Roche Diagnostics Corp., Indianapolis, IN) was used for preparation of DNA probes, and Southern hybridization was carried out as per manufacturer instructions.

Construction of Δ*ttnD* and Δ*ttnF* Mutant Strains SB13013 and SB13014. The *ttnD* and *ttnF* genes were inactivated by application of REDIRECT Technology according to the literature protocols.[6,29] An apramycin (Apr) resistance gene *aac(3)IV/oriT* cassette was used to replace an internal region of each target gene. Mutant cosmids pBS13025 (Δ*ttnD*) and pBS13026 (Δ*ttnF*) for gene inactivation were constructed (Table S1, Supporting Information) and then introduced into *S. griseochromogenes* by conjugation from *E. coli* ET12567/pUZ8002 according to the literature procedure with the following modifications.[6,29,30] Thus, *S. griseochromogenes* spores were suspended in TSB medium and heat-shocked at 45 °C for 15 min, followed by incubation at 30 °C for 6 h. Germinated spores (as conjugation recipients) were mixed with *E. coli* ET12567/pUZ8002 harboring mutant cosmid (as conjugation donor) and spread onto modified ISP-4 plates freshly supplemented with 20 mM MgCl₂. After incubation at 28 °C for 16−22 h, each plate was overlaid with 1 mL of sterilized water containing Apr at a final concentration of 10 μg/mL and nalidixic acid at a final concentration of 50 μg/mL. Incubation continued at 28 °C until exconjugants appeared. The double-crossover mutants found to be apramycin resistant and kanamycin sensitive were selected, named SB13013 (Δ*ttnD*) and SB13014 (Δ*ttnF*), and verified by PCR and subsequently confirmed by Southern analysis (Figures S1 and S2, Supporting Information).

Complementation of the Δ*ttnD* Mutation in SB13013 and the Δ*ttnF* Mutation in SB13014. To construct expression plasmids for genetic complementation experiments, *ttnD* and *ttnF* were amplified and digested by *Nsi*I and *Xba*I and then cloned into the same sites of pBS6027[7] to give pBS13029 (for *ttnD* expression) and pBS13030 (for *ttnF* expression). They were introduced into

the corresponding mutant strains by conjugation to yield complemented strains SB13015 (i.e., SB13103/pBS13029) and SB13016 (i.e., SB13104/pBS13030), respectively (Table S3, Supporting Information).

Fermentation of S. griseochromogenes Wild-Type and Recombinant Strains and Production of TTN and Analogues. A two-stage fermentation procedure was utilized to grow the *S. griseochromogenes* wild-type and recombinant strains SB13013, SB13014, SB13015, and SB13016 for TTN and analogue production as previously described.[6] Thus, seed medium (50 mL in a 250-mL flask) was inoculated with spores, and the flasks were incubated on a rotary shaker at 250 rpm (Innova44 Incubator Shaker Series, New Brunswick Scientific Co., Inc., Edison, NJ) and 28 °C for 2 days. This seed culture (50 mL) was then transferred into the fermentation medium (500 mL in a 2-L flask), and the flasks were incubated on a rotary shaker at 250 rpm and 28 °C for 5 days. Both seed and production media consist of glucose 2% (separately autoclaved), soluble starch 0.5%, beef extract 0.05%, yeast extract 0.3%, soybean flour 1%, NaCl 0.1%, K₂HPO₄ 0.0025%, and distilled water and tap water (1:1), pH 7.0, and were sterilized by autoclaving at 121 °C for 35 min.

Extraction and Isolation of TTN (1) and Analogues 3−7 from S. griseochromogenes Fermentation. The typical procedure for extraction and isolation of TTN and analogues from *S. griseochromogenes* wild-type and recombinant strain fermentation is as follows. The fermentation broth (10 L) was harvested by first bringing the broth pH to 4.0 via dropwise addition of 1 N HCl. Fermentation mixtures were then centrifuged at 3800 rpm (SLC-6000 rotor, Sorvall Evolution RC, Thermo Scientific Inc., Waltham, MA) at 4 °C for 20 min to pellet the mycelia. Broth supernatants were then collected and filtered to afford transparent amber-colored supernatants. Supernatants were then adsorbed onto 1.8 L of XAD-16 resin twice. Resins (now bearing secondary metabolites) were then washed with 5.4 L of distilled water to remove residual cells and broth components and then subjected to 3.6 L of acetone to elute the absorbed compounds. Acetone was removed under vacuum to give the crude products, and these products were then dissolved into 600 mL of acidic water (pH 4.0). Acidic aqueous fractions were then extracted three times with 900 mL of ethyl acetate (300 mL of fresh solvent each time). The resulting organic layers were combined and dried over anhydrous sodium sulfate. Following removal of all solids, the ethyl acetate was removed under reduced pressure to afford the crude syrups containing TTN and analogues. The syrups were then subjected to column chromatography over silica gel 60 RP-18, eluted with acetonitrile and water (from 2:8 to 9:1; 300 mL each) gradient. Each 100 mL fraction was analyzed by analytical HPLC, employing a detection wavelength of 264 nm and a linear gradient running from a buffer A/buffer B composition of 70:30 to 100% buffer B over the course of 24 min and continued at 100% buffer B for an additional 3 min, at a flow rate of 1 mL/min. Fractions containing TTN or analogues were combined and the solvents removed under reduced pressure for further purification by HPLC on an analytic or semi-preparative C-18 column. Precise purification procedures for each compound are noted below. Following collection of relevant fractions from HPLC, samples were frozen in dry ice and then solvent lyophilized for 12 h.

For purification of TTN (**1**) and TTN F-1 (**3**), semi-preparative HPLC was carried out on an Alltech Alltima C-18 column (250 × 10.0 mm, 5 μm), employing a linear gradient from buffer A/buffer B (70:30) to 100% buffer B over 24 min and continued at 100% buffer B for an additional 3 min, at a flow rate of 3 mL/min and monitored by UV detection at 264 nm.

For purification of TTN D-1 (**4**), the linear gradient went from buffer A/buffer B (90:10) to 100% buffer B over 20 min and continued at 100% buffer B for an additional 3 min, at a flow rate of 3 mL/min and monitored by UV detection at 264 nm.

For purification of diastereomers **5** and **6**, an effective linear gradient involved ramping from buffer A/buffer B (60:40) to buffer A/buffer B (20:80) over 16 min with continued flow at 100% buffer

(28) Paget, M. S.; Chamberlin, L.; Atrih, A.; Foster, S. J.; Buttner, M. J. *J. Bacteriol.* **1999**, *181*, 204–211.

(29) Gust, B.; Challis, G. L.; Fowler, K.; Kieser, T.; Chater, K. F. *Proc. Natl. Acad. Sci. U.S.A.* **2003**, *100*, 1541–1546.

(30) Kieser, T.; Bibb, M. J.; Buttner, M. J.; Chater, K. F.; Hopwood, D. A. *Practical Streptomyces Genetics*; John Innes Foundation: Norwich, UK, 2000.

(31) Liu, W.; Shen, B. *Antimicrob. Agents Chemother.* **2000**, *44*, 382–392.

B for an additional 2 min, at a flow rate of 3 mL/min and UV detection at 264 nm. The first peak corresponded to compound **5**, and the slightly slower-moving peak corresponded to compound **6**.

For purification of TTN D-4 (**7**), the linear gradient went from buffer A/buffer B (70:30) to 100% buffer B over 16 min and continued at 100% buffer B for an additional 2 min, at a flow rate of 3 mL/min and monitored by UV detection at 264 nm.

TTN F-1 (3). Absolute yield: 16 mg from 16 L of fermentation broth of SB13014. Yellowish gum; $[\alpha]_D^{25} = +22.9$ (*c* 1.0, acetone); APCI-MS (positive mode) *m/z* 637 ([M − H$_2$O + H]$^+$, 15), 619 ([M − 2H$_2$O + H]$^+$, 50), 601 ([M − 3H$_2$O + H]$^+$, 15), 281 (80), 263 (100), and 139 (65); HR-ESI-MS (negative mode) *m/z* 653.3532 [M − H]$^-$ (calcd for C$_{34}$H$_{53}$O$_{12}$, 653.3543, −1.6 ppm error); IR 3415, 2930, 1766, 1707, 1457, 1427, 1364, 1269, 1225, 1180, 1110, 1073, 1048, 910, 824, 794, and 706 cm^{-1}. For ^{1}H and ^{13}C NMR data, see Table 1.

TTN D-1 (4). Absolute yield: 17 mg from 40 L of fermentation broth of SB13013. Off-yellowish gum; $[\alpha]_D^{25} = +20.0$ (*c* 1.0, acetone); APCI-MS (negative mode) *m/z* 635 ([M − H]$^-$, 100); HR-MALDI-MS (positive mode) *m/z* 659.3412 [M + Na]$^+$ (calcd for C$_{34}$H$_{52}$O$_{11}$Na, 659.3402, 1.58 ppm error); IR 3422, 2930, 1766, 1706, 1621, 1515, 1456, 1364, 1259, 1222, 1177, 1089, 1062, 1029, 985, 907, 852, 764, and 731 cm^{-1}. For ^{1}H and ^{13}C NMR data, see Table 1.

TTN D-2 (5). Absolute yield: 30 mg from 40 L of fermentation broth of SB13013. Off-yellowish gum; $[\alpha]_D^{25} = +12.0$ (*c* 2.0, acetone); APCI-MS (negative mode) *m/z* 651 ([M − H]$^-$, 100); HR-ESI-MS (negative mode) *m/z* 651.3400 [M − H]$^-$ (calcd for C$_{34}$H$_{51}$O$_{12}$, 651.3375, 3.83 ppm error); IR 3407, 2931, 1830, 1765, 1703, 1621, 1456, 1365, 1260, 1223, 1179, 1032, 986, 957, 907, 854, and 732 cm^{-1}. For ^{1}H and ^{13}C NMR data, see Table 2.

TTN D-3 (6). Absolute yield: 12 mg from 40 L of fermentation broth of SB13013. Off-yellowish gum; $[\alpha]_D^{25} = +21.8$ (*c* 1.0, acetone); APCI-MS (negative mode) *m/z* 651 ([M − H]$^-$, 100); HR-ESI-MS (negative mode) *m/z* 651.3399 [M − H]$^-$ (calcd for C$_{34}$H$_{51}$O$_{12}$, 651.3375, 3.68 ppm error); IR 3406, 2961, 1830, 1765, 1703, 1621, 1456, 1365, 1260, 1223, 1179, 1040, 985, 956, 908, 855, and 732 cm^{-1}. For ^{1}H and ^{13}C NMR data, see Table 2.

TTN D-4 (7). Absolute yield: 4 mg from 40 L of fermentation broth of SB13013. Off-yellowish gum; $[\alpha]_D^{25} = +12.0$ (*c* 2.0, acetone); APCI-MS (negative mode) *m/z* 649 ([M − H]$^-$, 100); HR-ESI-MS (negative mode) *m/z* 649.3239 [M − H]$^-$ (calcd for C$_{34}$H$_{49}$O$_{12}$, 649.3219, 3.15 ppm error); IR 3416, 2966, 1829, 1765, 1704, 1625, 1581, 1457, 1378, 1261, 1181, 1090, 1033, 986, 957, 908, and 732 cm^{-1}. For ^{1}H and ^{13}C NMR data, see Table 1.

Supporting Information Available: Full experimental details describing production and confirmation of Δ*ttnD* and Δ*ttnF* mutant strains SB13013 and SB13014 and ^{1}H and ^{13}C NMR spectra for new TTN analogues **3**−**7**. This material is available free of charge via the Internet at http://pubs.acs.org.

JA9082446